Makara Journal of Science

Volume 27
Issue 2 *June*

Article 5

6-25-2023

Equilibrium and Kinetic Studies of Crude Oil Sorption on Unmodified and Modified Napier Grass

Amalachukwu Ifeyinwa Obi
Department of Pure and Industrial Chemistry, Nnamdi Azikiwe University Awka, Anambra State 420007, Nigeria, ai.obi@unizik.edu.ng

Vincent Ishmael Ajiwe
Department of Pure and Industrial Chemistry, Nnamdi Azikiwe University Awka, Anambra State 420007, Nigeria

Chinwe Priscilla Okonkwo
Department of Pure and Industrial Chemistry, Nnamdi Azikiwe University Awka, Anambra State 420007, Nigeria

Recommended Citation

Obi, Amalachukwu Ifeyinwa; Ajiwe, Vincent Ishmael; and Okonkwo, Chinwe Priscilla (2023) "Equilibrium and Kinetic Studies of Crude Oil Sorption on Unmodified and Modified Napier Grass," *Makara Journal of Science*: Vol. 27: Iss. 2, Article 5.
DOI: 10.7454/mss.v27i2.1458
Available at: https://scholarhub.ui.ac.id/science/vol27/iss2/5

Makara Journal of Science, 27/2 (2023), 115–128
doi: 10.7454/mss.v27i2.1458

Equilibrium and Kinetic Studies of Crude Oil Sorption on Unmodified and Modified Napier Grass

Amalachukwu Ifeyinwa Obi*, Vincent Ishmael Ajiwe, and Chinwe Priscilla Okonkwo

Department of Pure and Industrial Chemistry, Nnamdi Azikiwe University Awka, Anambra State 420007, Nigeria

*E-mail: ai.obi@unizik.edu.ng

Received November 8, 2022 | Accepted April 8, 2023

Abstract

Nowadays, natural organic adsorbents are widely used to clean up oil from spills owing to their effectiveness, affordability, and biodegradability. In this study, Napier grass, a widely available agricultural material, was used to remove crude oil from aqueous media. The Napier grass was modified via a mild acetylation process to improve its hydrophobicity. The modification increased the Brunauer–Emmett–Teller surface area of the grass from 180.07 to 271.13 m^2/g. Fourier-transform infrared analysis revealed that the modification endowed the originally hydrophilic Napier grass with hydrophobicity. The oil sorption processes were based on monolayer physisorption and controlled by film diffusion. The oil sorption capacities of the unmodified and modified Napier grass under various adsorption conditions (adsorbent dose, initial crude oil concentration, and contact time) were significantly different. The equilibrium oil sorption capacities of the unmodified and modified grass were 7070 and 9057 mg/g, respectively, reflecting the improvement of oil sorption capacity by the modification process. These results indicate that the modification process significantly improved the crude oil adsorption ability of Napier grass. Thus, acetylated Napier grass is an effective, readily available oil sorbent with application potential for the cleanup of crude oil spills.

Keywords: acetylation, Napier grass, oil adsorption

Introduction

Crude oil is a significant energy source and raw material for various products; thus, there is an increasing daily demand for it. This increase in demand leads to increased crude oil output and global transportation, which increases the risk of oil spills in the environment. This spillage can result from operational mistakes, broken equipment, accidents during transportation, natural calamities, mismanaged landfills, leaky reservoirs, or inappropriate crude oil handling. Crude oil spills release hazardous substances into the environment and thus can adversely affect plants, animals, and humans [1, 2]. Hence, research is ongoing to create effective oil spill remediation methods. The natural adsorption method, which employs cheap agricultural wastes and materials, is preferred because it is simple, efficient, and affordable, and the sorbents are biodegradable and renewable [3–5]. The sorbents, which are usually hydrophilic by nature, are modified to increase their hydrophobicity. Acetylation is one of the most employed chemical modification methods, because of its simplicity, cost-effectiveness, and efficiency in improving the hydrophobicity of natural fiber surfaces [6]. Moreover, moderate acetylation does not alter the natural crystalline structure of cellulose, allowing for the retention of desirable qualities [7]. Modification by acetylation leverages the fact that the hydroxyl functional group, which is hydrophilic, is the most reactive and abundant site in the cell wall polymers of most lignocellulosic materials. Therefore, reducing the density of the hydroxyl functional groups will increase the efficiency of these materials in a saturated aquatic environment [8]. By replacing the hydroxyl groups in the cell wall fibers with acetyl groups from acetic anhydride, the acetylation process converts the hydrophilic features of cellulosic materials into hydrophobic properties [9]. Agricultural materials such as corn silk [10], Delonix regia pods [11], corncob [12], sugarcane bagasse [13], oil palm empty fruit bunch, cocoa pods [14], and *Dacryodes edulis* leaves [15] have all been acetylated to increase their hydrophobicity for oil sorption applications. Although these acetylated sorbents efficiently adsorb crude oil, the plants that serve as their source require a lengthy growth time. Moreover, the preparation of the sorbents involves many processes that require a significant amount of time and energy. These limitations restrict the application of the sorbents for oil spill treatment. The preparation of sorbents using an environmentally friendly quick-growing biomaterial that requires few processes has attracted research attention. Napier grass is a perennial grass that spreads quickly through asexual reproduction,

with a high productivity of 87 tons/ha/year [16]. It is frequently discarded because many people regard it as a weed. It is, however, used as forage for livestock and for protection against erosion in some environments [17].

Several studies have investigated various possible applications of Napier grass, including biofuel production, corrosion inhibition, and the adsorption of dyes and heavy metals. However, to the best of our knowledge, there have been no reports on its modification by acetylation for crude oil adsorption. The aim of this study was to investigate the crude oil sorption behavior of unmodified Napier grass (UNG) and modified Napier grass (MNG). The effects of different adsorption conditions, such as adsorbent dose, contact time, and initial crude oil concentration were determined. Sorption equilibrium and kinetics were also studied using various isotherm and kinetic models.

Materials and Methods

Napier grass was gathered in Awka, a city in Anambra State, Nigeria. The gathered grass was thoroughly washed with clean water to remove dust and extraneous materials. The washed grass was dried under sunlight for about 12 h and then left to dry properly in an oven at 65 °C. The dried samples were ground using a manual grinding machine and sieved. The particles that passed through size 25 British standard sieves were collected and used for further analysis. Crude oil was obtained from the Port Harcourt Refinery in Rivers State, Nigeria. The crude oil belonged to the class of medium crudes, with a density of 898 kg/m^3 and an API gravity of 25.897°. The chemicals for this research were obtained from British Drug Houses, Ltd.

Modification of Napier grass. To minimize the impact of fiber extracts on acetylation, soxhlet extraction was performed on the Napier grass. A weighed portion (10 g) of the sieved Napier grass was exposed to a 4:1 v/v solution of n-hexane and acetone for 5 h. After the treated materials were dried, they were subjected to mild acetylation with acetic anhydride in the presence of 1% iodine as a catalyst using the method reported by Nwadiogbu *et al*. [18]. For this, 60 mL of acetic anhydride and 3 g of Napier grass were combined and heated to 30 °C for 1 h in a solvent-free system. The acetylated material was then dried and cooled before analysis.

Characterization of Napier grass. The surface areas, pore volumes, and pore sizes of UNG and MNG were measured using a Brunauer–Emmett–Teller (BET) analyzer (Quantachrome NOVA 4200e). The Fourier-transform infrared (FTIR) spectra of the sorbents were acquired before and after crude oil sorption using a Nicolet iS5 spectrometer in the spectral range of 4000–400 cm^{-1} in the attenuated total reflection mode.

Oil sorption test. The crude oil used for the sorption test was left in a beaker for 24 h in the open air to release volatile hydrocarbon content, simulating an oil spill. The oil sorption capacities of UNG and MNG were determined using a batch oil sorption technique. First, 10 g of the weathered crude oil was displaced in 100 mL of water and contacted with each adsorbent in a weighted fraction of 0.2 g. Then, with only minimum stirring, the mixture was maintained at 26 °C for five min. Then, the sorbent was allowed to drain through a mesh filter, dried at 60 °C, and reweighed. The oil sorption capacity (g/g) of the adsorbents was determined using Equation 1.

$$\text{Oil sorption capacity} = \frac{W_1 - W_0}{W_0} \quad (1)$$

W_0 and W_1 are the weights of the adsorbent in grams before and after crude oil sorption, respectively. Using the following mass balance equation, the equilibrium amount of crude oil adsorbed per unit weight of adsorbent, q_e (mg/g), was calculated:

$$q_e = \frac{(C_o - C_e)\cdot V}{m} \quad (2)$$

C_e and C_o (mg/L) are the equilibrium and initial concentrations of crude oil, respectively; m (g) is the mass of the adsorbent; and V is the volume of the solution in liters.

To study the effect of the adsorbent dose on the oil sorption capacities of UNG and MNG, the above procedure was conducted using 0.2, 0.4, 0.6, 0.8, and 1.0 g of each adsorbent under operating conditions of 26 °C, five min contact time, and crude oil concentration of 100 g/L. The impact of the initial oil concentration on the sorption capacity of the adsorbents was studied using crude oil concentrations of 50, 75, 100, 125, and 150 g/L under working conditions of 26 °C, 0.2 g adsorbent, and 5 min contact time. Data obtained from this study were used for equilibrium studies of the adsorption processes using various isotherm models. The effect of contact time on the oil sorption capacity of the adsorbents was determined through sorption experiments under contact times of 1, 3, 5, 10, and 15 min, with operating conditions of 26 °C, 0.2 g adsorbent, and crude oil concentration of 100 g/L. The data obtained were inputted into various kinetic models for kinetic analyses of the adsorption processes.

Adsorption isotherm. Four adsorption isotherm models—Langmuir, Freundlich, Temkin, and Dubinin–Radushkevich (D-R)—were used to examine the equilibrium of the adsorption processes.

Langmuir isotherm. The Langmuir isotherm model describes monolayer adsorbate coverage on an adsorbent, and is given as follows [15].

$$q_e = \frac{q_m \cdot b \cdot C_e}{1 + b \cdot C_e} \quad (3)$$

C_e is the equilibrium concentration of the adsorbate (g/L), q_m and q_e are the monolayer and equilibrium sorption capacities (g/g), respectively, and b is the Langmuir constant (L/g). The linear form of the isotherm is as follows [19].

$$\frac{C_e}{q_e} = \frac{1}{b \cdot q_m} + \frac{C_e}{q_m} \quad (4)$$

Plotting C_e/q_e against C_e results in a straight line graph, from whose slope and intercept q_m and b can be deduced, respectively.

Freundlich isotherm. The Freundlich isotherm, which applies to multilayer sorption on heterogeneous surfaces, is given as follows [20]:

$$q_e = K_F \cdot C_e^{1/n} \quad (5)$$

K_F is the Freundlich constant, which reflects the relative adsorption capacity of the adsorbent, and $^1/_n$ is a measure of the adsorption intensity; it describes the heterogeneity of the adsorbent site and the energy of distribution. The linearized isotherm is as follows [21]:

$$\ln q_e = \ln K_F + \frac{1}{n} \ln C_e \quad (6)$$

The intercept and slope of a linear plot of ln q_e as a function of ln C_e yield the K_F and n values, respectively.

Temkin isotherm. The Temkin isotherm, provided in Equation (7), assumes that owing to indirect adsorbate–adsorbent interactions, the adsorption energy decrease linearly with increasing surface coverage of the adsorbent [22].

$$q_e = B \ln(A \cdot C_e) \quad (7)$$

$$B = \frac{RT}{b} \quad (8)$$

A is the equilibrium binding constant (L/g), b is the Temkin constant related to the heat of adsorption (J/mol), T (K) is the absolute temperature, and R is the universal gas constant (8.314 J/mol. K). The isotherm's linear form is as follows [23]:

$$q_e = B \ln A + B \ln C_e \quad (9)$$

The slope and intercept of a straight line graph created by plotting q_e as a function of ln C_e yield the constants B and A, respectively.

D–R isotherm. The D–R isotherm, which assumes a multilayer character of adsorbate molecules involving van der Waals forces, is shown in nonlinear and linear forms in Equations (10) and (11) [24].

$$q_e = q_m \exp(-K_D \varepsilon^2) \quad (10)$$

$$\ln q_e = \ln q_m - K_D \varepsilon^2 \quad (11)$$

$$\varepsilon = RT \ln\left(1 + \frac{1}{C_e}\right) \quad (12)$$

K_D is the D–R constant (mol^2/kJ^2), ε is the Polanyi potential, and q_m is the maximum adsorption capacity (g/g). A straight line whose slope and intercept are $-K_D$ and ln q_m, respectively, results from plotting ln q_e versus ε^2.

Adsorption kinetics. To better comprehend the mechanism of the sorption processes, six kinetic models were applied: pseudo-first-order, pseudo-second-order, Elovich, intra-particle diffusion, and Boyd kinetic models.

Pseudo-first-order kinetic model. The pseudo-first-order kinetic equation is presented in Equation (13) [25].

$$\frac{dq_t}{dt} = k_1 \left(q_e - q_t\right) \quad (13)$$

q_e and q_t (mg/g) are the oil sorption capacities at equilibrium and time t (min), respectively, and k_1 is the pseudo-first-order reaction rate constant (min^{-1}). On integration and linearization, the model becomes Equation (14) [23].

$$\ln\left(q_e - q_t\right) = \ln q_e - k_1 t \quad (14)$$

A plot of ln (q_e–q_t) versus t gives a straight line with the slope and intercept as $-k_1$ and ln q_e, respectively. Conformity to the model indicates that the adsorption process involves physisorption [14].

Pseudo-second-order kinetic model. The pseudo-second-order model relies on the assumption of the chemisorption of the adsorbate on the adsorbent, and its nonlinear and linear forms are represented in Eqs. (15) and (16), respectively [26].

$$\frac{dq_t}{dt} = k_2 \left(q_e - q_t\right)^2 \quad (15)$$

$$\frac{t}{q_t} = \frac{1}{k_2 \cdot q_e^2} + \frac{t}{q_e} \quad (16)$$

K_2 is the pseudo-second-order reaction rate constant (g/mg·min). Plotting t/q_t as a function of t yields a straight line that gives k_2 from the intercept and q_e from the slope.

The Elovich model. The Elovich model, also based on the assumption that the adsorbate will become chemisorbed to the adsorbent, is given in nonlinear and linear forms in Eqs. (17) and (18), respectively [27].

$$\frac{dq_t}{dt} = \alpha \exp\left(-\beta q_t\right) \quad (17)$$

$$q_t = \frac{1}{\beta}\ln(\alpha\beta) + \frac{1}{\beta}\ln t \quad (18)$$

α (mg/g.min) is the initial adsorption rate, and β (g/mg) is the desorption constant related to the degree of surface coverage and activation energy for chemisorption. The intercept and slope of a linear plot of q_t versus ln t are employed to determine α and β, respectively.

Intra-particle diffusion model. This model, which describes an adsorption process based on intra-particle diffusion, is expressed by Equation (19) [28]

$$q_t = K_{id} \cdot t^{1/2} + l \quad (19)$$

K_{id} is the rate constant of intra-particle diffusion (mg/g·min$^{1/2}$), and l is the estimated thickness of the boundary layer. The slope and intercept of a plot of q_t versus $t^{1/2}$ yield K_{id} and l, respectively. If the plot of q_t versus $t^{1/2}$ results in a straight line passing through the origin, then intra-particle diffusion is the mechanism behind the sorption process [23].

Boyd model. The Boyd kinetic equation is expressed as follows [29]:

$$F = 1 - \left(\frac{6}{\pi^2}\right)\exp(-B_t) \quad (20)$$

where $F\left(=\frac{q_t}{q_e}\right)$ is the fractional attainment of equilibrium, and B_t is a mathematical function of F. Substitution for F in Equation (20) and rearranging the equation yields Equation (21).

$$B_t = -0.4977 - \ln(1 - F) \quad (21)$$

If a plot of B_t as a function of time gives a straight line passing through the origin, then intra-particle diffusion controls the adsorption; otherwise, film diffusion or external mass transfer controls it [30].

Statistical analysis. A paired sample t-test with a 95 % confidence interval in Statistical Package for Social Sciences version 26 was employed to compare the adsorption capacities of UNG and MNG. *P*-values below the 0.05 significance level indicate significant changes in the mean values.

Results and Discussion

Surface area analysis of the adsorbents. The N_2 adsorption isotherm plots for UNG and MNG are presented in Figures 1 and 2, respectively. The modified grass exhibited larger BET and Barrett–Joyner–Halenda (BJH) surface areas (271.13 and 345.70 m^2/g, respectively) than the unmodified grass (180.07 and 203.00 m^2/g, respectively). In accordance with the International Union of Pure and Applied Chemistry (IUPAC) classification, the isotherms resemble a combination of type I and II isotherms. This indicates a combination of microporous- and mesoporous structures [31]. The pore sizes are divided into three categories according to the IUPAC criteria: micropores (less than 20 Å or 2 nm), mesopores (between 20 Å or 2 nm and 500 Å or 50 nm), and macropores (greater than 500 Å or 50 nm) [32]. The pore size distribution curves for both UNG and MNG featured the sharpest peak between pore diameters 2 and 3 nm. The average BJH pore sizes of UNG and MNG were 2.122 and 2.072 nm, respectively, while the Dubinin–Astakhov pore sizes were 2.740 and 2.940 nm, respectively. This shows that the UNG and MNG were dominated by mesopores. The modification process increased the pore volume from 0.0992 to 0.1668 cc/g. The increments in surface area and pore volume are attributable to the replacement of low-weight hydroxyl groups with bulkier acetyl groups from acetic anhydride during the acetylation process, thereby increasing the active area [8]. The slight reduction in pore size was likely due to the swelling of the cell wall of the Napier grass during the acetylation process through the introduction of the bulky acetyl groups [33].

FTIR analysis. The FTIR spectra of UNG and MNG before and after crude oil sorption, are displayed in Figure 3. The UNG spectra show a broad absorption band with a center point at 3330 cm^{-1} and a narrow band in the range of 2852–2918 cm^{-1}, which correspond to O–H and C–H vibrations, respectively [28]. The peak at 1641 cm^{-1} corresponds to the bending vibrations of H-O-H [34]. C–O stretching vibrations of ethers occurred at 1032–1320 cm^{-1}, and the peak at 897 cm^{-1} indicated the C–O rotational vibration of β–glycosidic linkages in polysaccharides [28]. The UNG spectra featured peaks corresponding to cellulose, hemicellulose, and lignin, indicating that Napier grass is a lignocellulosic material.

The MNG spectra featured a downward shift in the wavenumber of the absorption bands. The middle point of the O–H stretching band appeared at 3333 cm^{-1} in the UNG spectra but at 3326 cm^{-1} in the MNG spectra, while the C–H stretching band appeared at 2852–2918 cm^{-1} in the UNG spectra but at 2852–2901 cm^{-1} in the MNG spectra. The H--O-H bending vibration appeared at 1641 in the UNG spectra but at 1637 cm^{-1} in the MNG spectra. C–O stretching and glycosidic linkage appeared at 1320–1032 cm^{-1} and 897 cm^{-1}, respectively, in the UNG spectra, but at 1316–1032 cm^{-1} and 896 cm^{-1}, respectively, in the MNG spectra. These downward shifts in wavenumber in the MNG FTIR spectra compared with the UNG spectra are attributable to the modification process. The MNG spectra also showed an absorption peak at 1734 cm^{-1}, which corresponds to the C=O stretching of the acetyl group. The appearance of this peak and the reduction in the intensities of the other absorption peaks indicate the attachment of the acetyl

group from the acetic anhydride reagent to the Napier grass, which led to the removal of the weak components of hemicellulose and lignin present in the grass [19].

The spectra of the crude oil-treated sorbents featured intense peaks at 2852 cm^{-1} and enhanced peaks at 2921.65 cm^{-1} and 1456 cm^{-1}. These peaks correspond to the C–H stretching of the methylene and methyl groups and the C–H bending of crude oil, respectively [13]. The creation and enhancement of these peaks indicate that crude oil was adsorbed on the hydrophobic sites of the sorbents, consistent with the results of previous studies [13, 32]. The new and enhanced absorption peaks were more intense in the spectra of MNG after sorption (MNG-S) than in the spectra of UNG after sorption (UNG-S), indicating that MNG adsorbed more crude oil than UNG, owing to the presence of more hydrophobic sites. In contrast to MNG, UNG adsorbed much more water, as indicated by the enhanced peaks at 3332.17 cm^{-1} [35] and at 1634 cm^{-1} [36] in the FTIR spectra of UNG-S. These observations demonstrate that the modification endowed the originally hydrophilic Napier

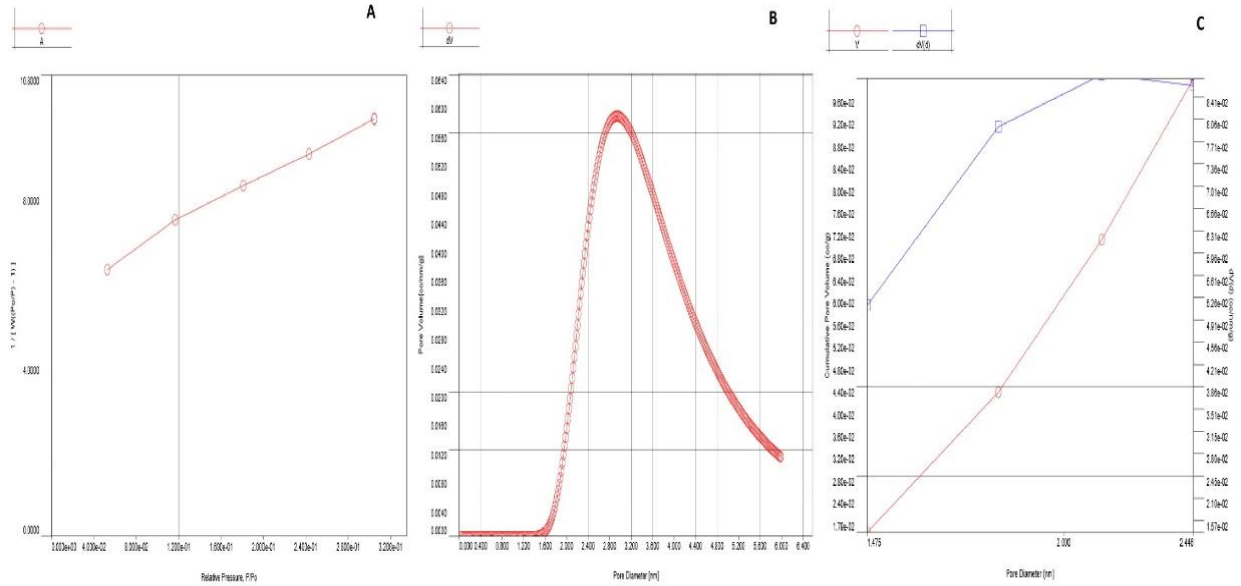

Figure 1. Nitrogen Adsorption Isotherm and Pore Size Distributions of Unmodified Napier Grass

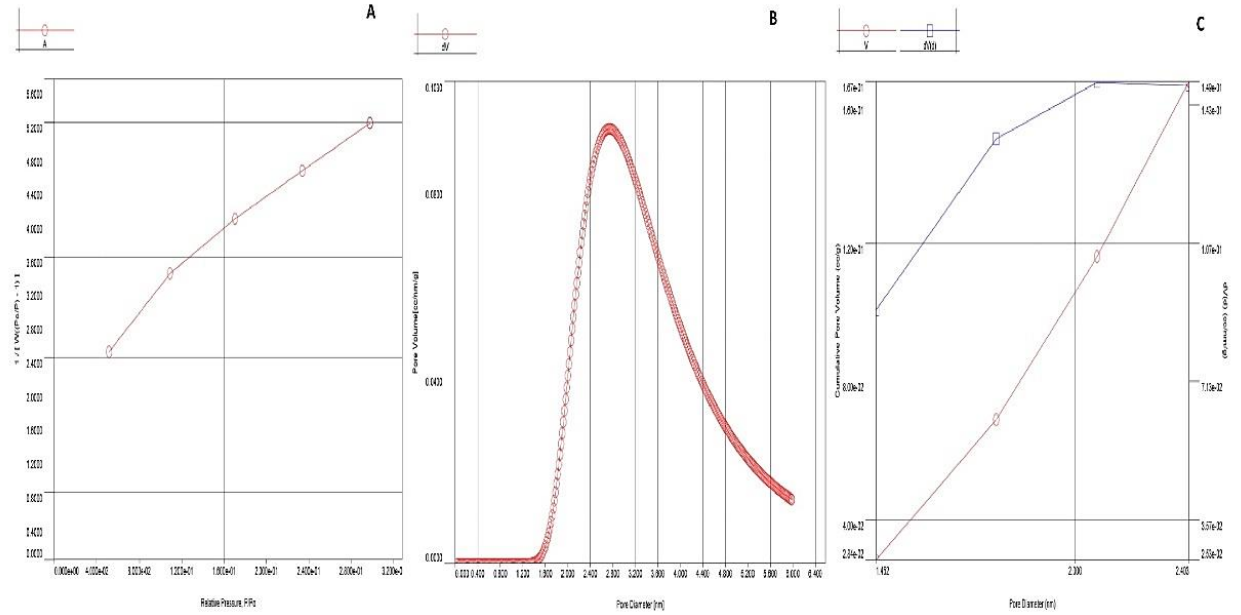

Figure 2. Nitrogen Adsorption Isotherm and Pore Size Distributions of Modified Napier Grass

grass with hydrophobicity. Figure 4 illustrates the proposed mechanism explaining the observations. The hydroxyl groups on the UNG surface possibly repelled the crude oil molecules in the sorption medium but attracted water molecules [37]. The introduction of acetyl groups from acetic anhydride during the modification process (Figure 4a) led to the creation of a nonpolar layer on the Napier grass surface, and crude oil molecules were attached to the layer (Figure 4b). The increase in the hydrophobicity and the active area of the Napier grass enhanced and provided more active sites for higher oil uptake.

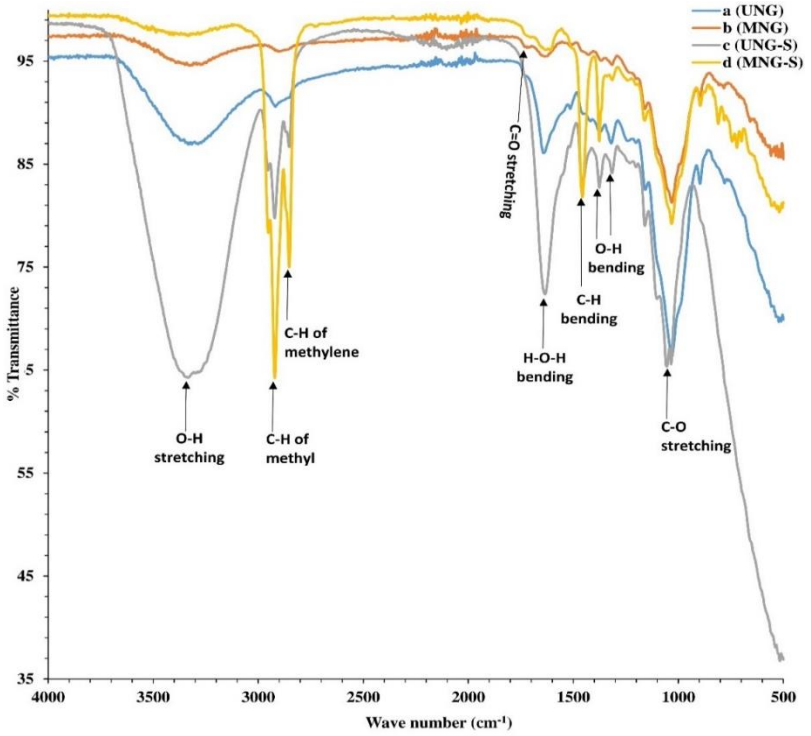

Figure 3. FTIR Spectra of Unmodified and Modified Napier Grass Before and After Sorption

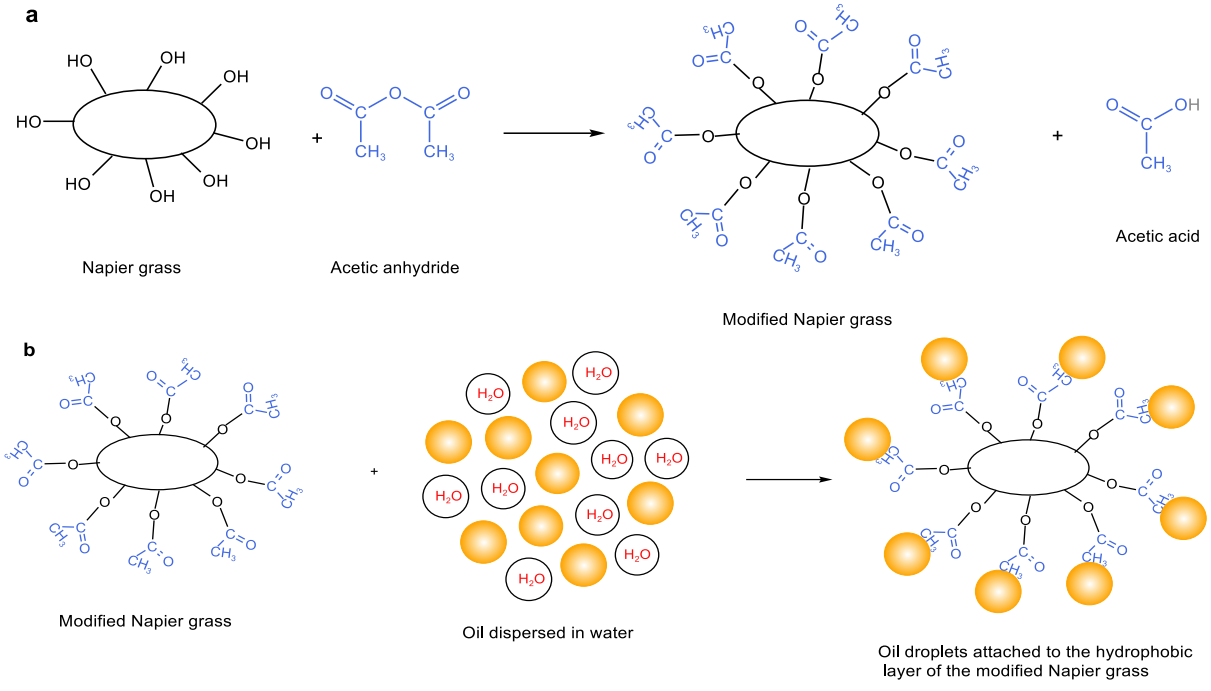

Figure 4. Proposed Mechanisms of Napier Grass Modification and Oil Adsorption

Effect of adsorbent dose on oil sorption capacity. Figure 5 shows the effects of the doses of UNG and MNG on their oil sorption capacities. With increasing sorbent dose from 0.2 to 1.0 g, the oil sorption capacities of UNG and MNG reduced from 5.414 to 4.276 g/g and 6.825 to 5.268 g/g, respectively. This decrease is attributable to the convergence of the sorption sites as the sorbent dose increased, which reduced the overall adsorption surface area and hence reduced the amount of sorbate adsorbed per unit gram of sorbent [38, 39]. For the various considered adsorbent doses, MNG demonstrated a higher oil sorption capacity than UNG. With increasing surface area of contact between the oil adsorbate and sorbent particles, the oil sorption capacity increased [40]. Consequently, more oil was adsorbed under a large surface area. Therefore, the higher sorption capacity of MNG is attributable to its larger surface area and pore volume. The higher oil sorption capacity of MNG also demonstrates its increased hydrophobicity.

Effect of initial crude oil concentration on oil sorption capacity. Figure 6 shows the impact of the initial crude oil concentrations on the oil sorption capacities of UNG and MNG. The oil sorption capacity of UNG increased with the increase in the initial crude oil concentration from 50 to 100 g/L. Further increase in the oil concentration resulted in lower oil sorption capacity. The oil sorption capacity of MNG increased with increasing initial oil concentration up to 125 g/L and then decreased. The oil sorption capacity increased with the initial oil concentration because the concentration gradient provided the requisite driving force for the mass transfer of adsorbate from the bulk phase to the adsorbent surface [13]. However, each adsorbent had a limited number of active sites, and the sites became saturated when exposed to higher concentrations of adsorbate, thereby causing a reduction in the sorption capacity [8]. Compared with MNG, UNG attained saturation at a lower crude oil concentration, indicating that acetylation produced more

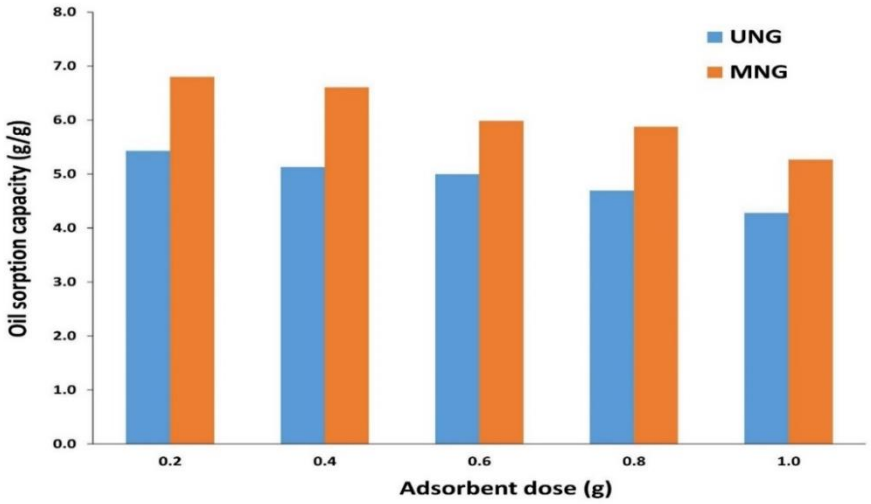

Figure 5. Effect of Adsorbent Dose on the Oil Sorption Capacities of Unmodified and Modified Napier Grass

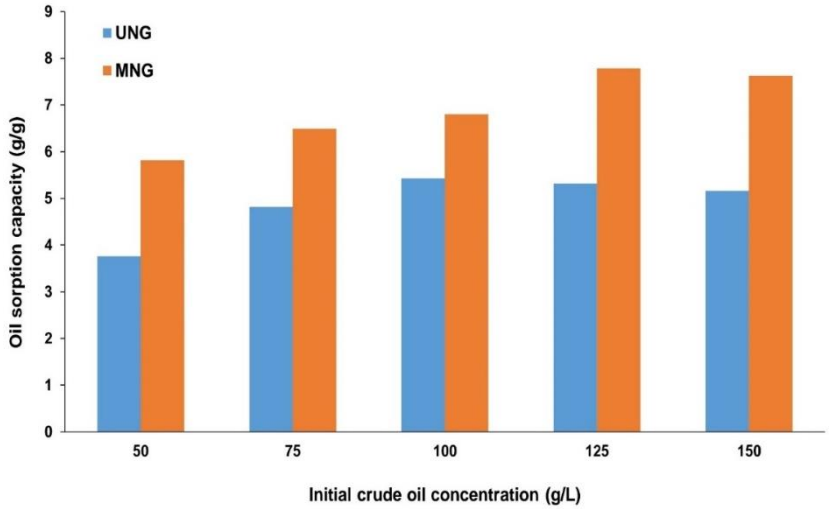

Figure 6. Effect of Initial Crude Oil Concentration on the Oil Sorption Capacities of Unmodified and Modified Napier Grass

active sites for oil sorption. For the various initial crude oil concentrations considered, MNG showed a higher oil sorption capacity than UNG, demonstrating the enhanced hydrophobicity of the former.

Isotherm study. The Langmuir, Freundlich, Temkin, and D–R plots for the adsorption of crude oil on UNG and MNG are shown in Figures 7 a, b, c, and d, respectively. The isotherm parameters obtained from the plots are listed in Table 1. The Langmuir isotherms had the highest R^2 values (>0.9700) among all of the applied isotherms for adsorption on UNG and MNG. This suggests that the Langmuir isotherm best described the crude oil sorption processes, which agrees with other reports [12, 41]. Conformity to the Langmuir isotherm implies that the adsorption processes involved monolayer coverage of the adsorbents by the crude oil. The theoretical monolayer sorption capacities (q_m) for UNG and MNG are 6.131 and 9.001 g/g, respectively.

According to the Langmuir isotherm, each sorbent has a limited number of uniform adsorption sites [42]. A higher q_m value obtained for MNG indicates that the modification process increased the number of sorption sites on the Napier grass, which increased the oil sorption capacity of the grass. The separation factor, R_L, represented in Equation (22), is a dimensionless constant used to determine the characteristics of a Langmuir-type adsorption process.

$$R_L = \frac{1}{1 + b \cdot C_o} \quad (22)$$

C-$_o$ is the initial adsorbate concentration (mg/L), and b is the Langmuir constant (L/mg). Adsorption is described as favorable, unfavorable, linear, or irreversible at $0 < R_L < 1$, $R_L > 1$, $R_L = 1$, or $R_L = 0$, respectively [25]. The R_L values for the adsorption on UNG and MNG obtained using various C_o values were between 0 and 1 (Table 1), indicating that the adsorption processes were favorable. Moreover, the n values obtained from the Freundlich isotherm for adsorption on UNG and MNG are between 1 and 10, indicating favorable adsorption [21].

The D–R constant, K_D provides insight into the mean free energy of adsorption, E (kJ/mol), which can be determined using the following relationship [23]:

$$E = \frac{1}{\sqrt{2K_D}} \quad (23)$$

Physical sorption occurs when the adsorption energy is less than 8 kJ/mol, while chemical sorption occurs when the energy is between 8 and 16 kJ/mol [43, 44]. For the adsorption of crude oil on UNG and MNG, the E values were 0.0707 and 0.0845 kJ/mol, respectively, which indicates the physical nature of the sorption processes. The b values obtained from the Temkin isotherm were 2.023 and 1.136 kJ/mol for the adsorption on UNG and MNG, respectively. Both values were less than 8 kJ/mol,

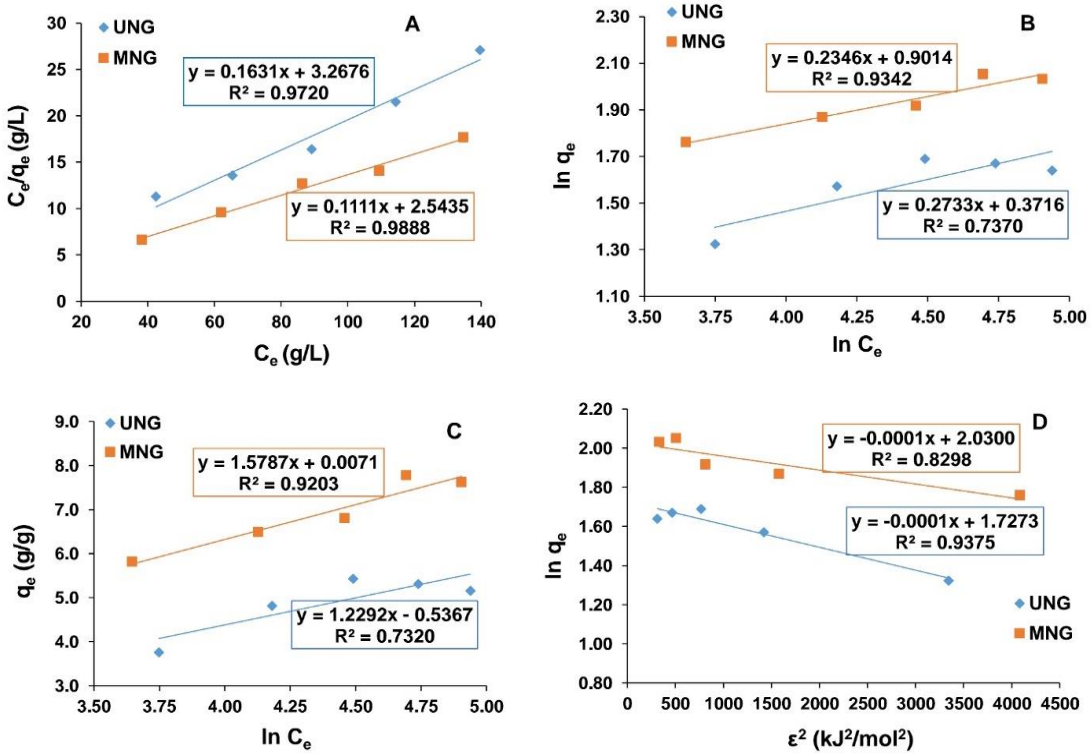

Figure 7. (a) Langmuir, (b) Freundlich, (c) Temkin, and (d) Dubinin–-Radushkevich Isotherms for Oil Sorption on Unmodified and Modified Napier Grass

Table 1. Isotherm Parameters for Oil Sorption on Unmodified and Modified Napier Grass

Parameter	UNG	MNG
Langmuir isotherm		
q_m (g/g)	6.131	9.001
b (L/g)	4.99×10^{-2}	4.37×10^{-2}
R_L	0.286–0.118	0.314–0.132
Freundlich isotherm		
K_F (L/g)	1.450	2.463
n	3.659	4.263
Temkin isotherm		
A (L/g)	0.646	1.005
B	1.2292	1.5787
b (kJ/mol)	2.022	1.575
Dubinin–Radushkevich isotherm		
q_m (g/g)	5.625	7.614
K_D (mol^2/kJ^2)	1×10^{-4}	7×10^{-5}

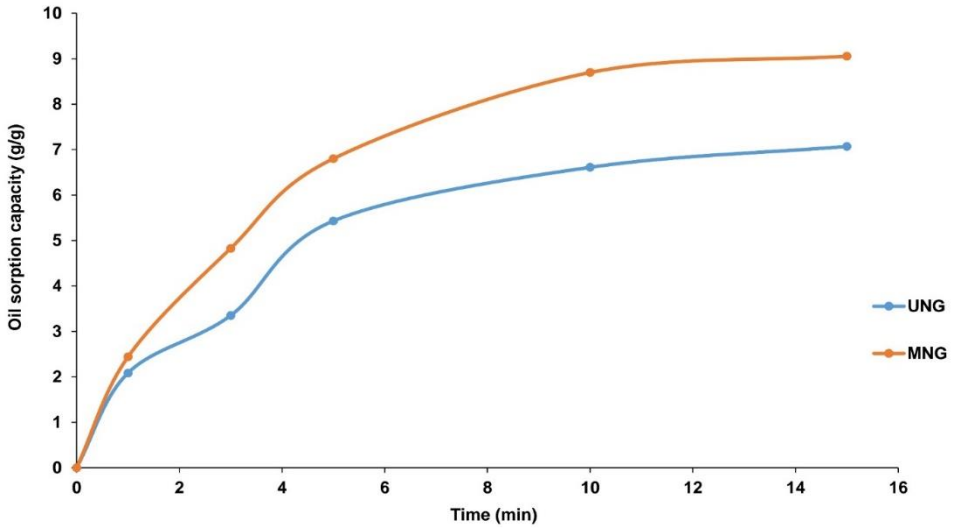

Figure 8. Effect of Contact Time on the Oil Sorption Capacities of Unmodified and Modified Napier Grass

showing that the adsorption processes were physisorption, consistent with previous reports on the physical nature of crude oil sorption onto lignocellulosic materials [12, 14].

Effect of contact time on oil sorption capacity. To study the kinetics of the sorption processes, the impact of time on the oil sorption capacities of UNG and MNG was investigated. Figure 8 shows that the oil sorption capacities of both sorbents increased with increasing contact time. The sorption processes started quickly but slowed down as they approached equilibrium, because there were a large number of empty surface sites and pores available for sorption in the beginning phases, but that number decreased as the sorption process advanced. The occurrence of repulsive forces between the adsorbed oil molecules and the molecules in the bulk phase may have also contributed to the reduced availability of sorption sites and pores [43]. The oil sorption capacity of MNG was higher than that of UNG throughout the considered sorption time. After 15 min of contact, the sorption processes approached equilibrium, and the sorption capacities of UNG and MNG were 7.070 and 9.057 g/g, respectively. The higher sorption capacity of MNG is attributable to its larger surface area and pore volume and enhanced hydrophobicity.

Kinetic study. The pseudo-first-order, pseudo-second-order, Elovich, intra-particle diffusion, and Boyd plots for crude oil adsorption on UNG and MNG are shown in Figures 9a, b, c, d, and e, respectively. The kinetic parameters obtained from the plots are listed in Table 2. The Elovich plots featured lower linear regression values (0.9601 and 0.9849 for UNG and MNG, respectively)

than the pseudo-first order and pseudo-second order plots. This indicates that the Elovich kinetic model is not suitable for describing the adsorption processes, suggesting that the adsorption mechanism was not chemisorption [24]. The pseudo-second-order and pseudo-first-order models provided very high R^2 values for the sorption processes. However, the q_e values provided by the pseudo-first-order model are closer to the experimentally obtained values for both UNG and MNG. This observation, along with the higher R^2 value for adsorption on UNG, suggests that the pseudo-first-order kinetic model provided a better fit for the sorption processes, which implies that the crude oil adsorption processes were physisorption. This agrees with the results of the mean energies of sorption, which indicated the physical nature of the sorption processes. Sorption on MNG proceeded at a higher rate than sorption on UNG, as reflected by the higher k_1 value obtained for sorption on MNG (Table 2). This shows that the modification of Napier grass increased its oil sorption rate. Table 3 compares the crude oil sorption capacity of MNG with those of some other acetylated lignocellulosic materials. The data show that MNG is an efficient low cost adsorbent for crude oil removal from aqueous media.

To determine the rate-controlling step of the sorption processes, intra-particle diffusion and Boyd kinetic models were applied. The lines in the intra-particle diffusion model graphs for UNG and MNG did not pass through the origin, showing that intra-particle diffusion was not the rate-controlling step of the oil sorption processes [23]. The non-zero intercepts of the graphs indicate the relevance of boundary layer diffusion. The higher intercept obtained in the plot for adsorption on MNG suggests that there was more boundary layer effect for adsorption on MNG than for adsorption on UNG. The higher k_{id} values obtained for adsorption on MNG than for adsorption on UNG reflect the improved adsorption potential of MNG. The Boyd kinetic model provided larger R^2 values than the intra-particle diffusion model, showing that film diffusion predominated over intra-particle diffusion. The non-zero intercept obtained from the Boyd kinetic model indicates that the sorption processes were controlled by film diffusion, which is the diffusion of the oil molecules from the bulk fluid to the external surface of the adsorbents across the boundary layer.

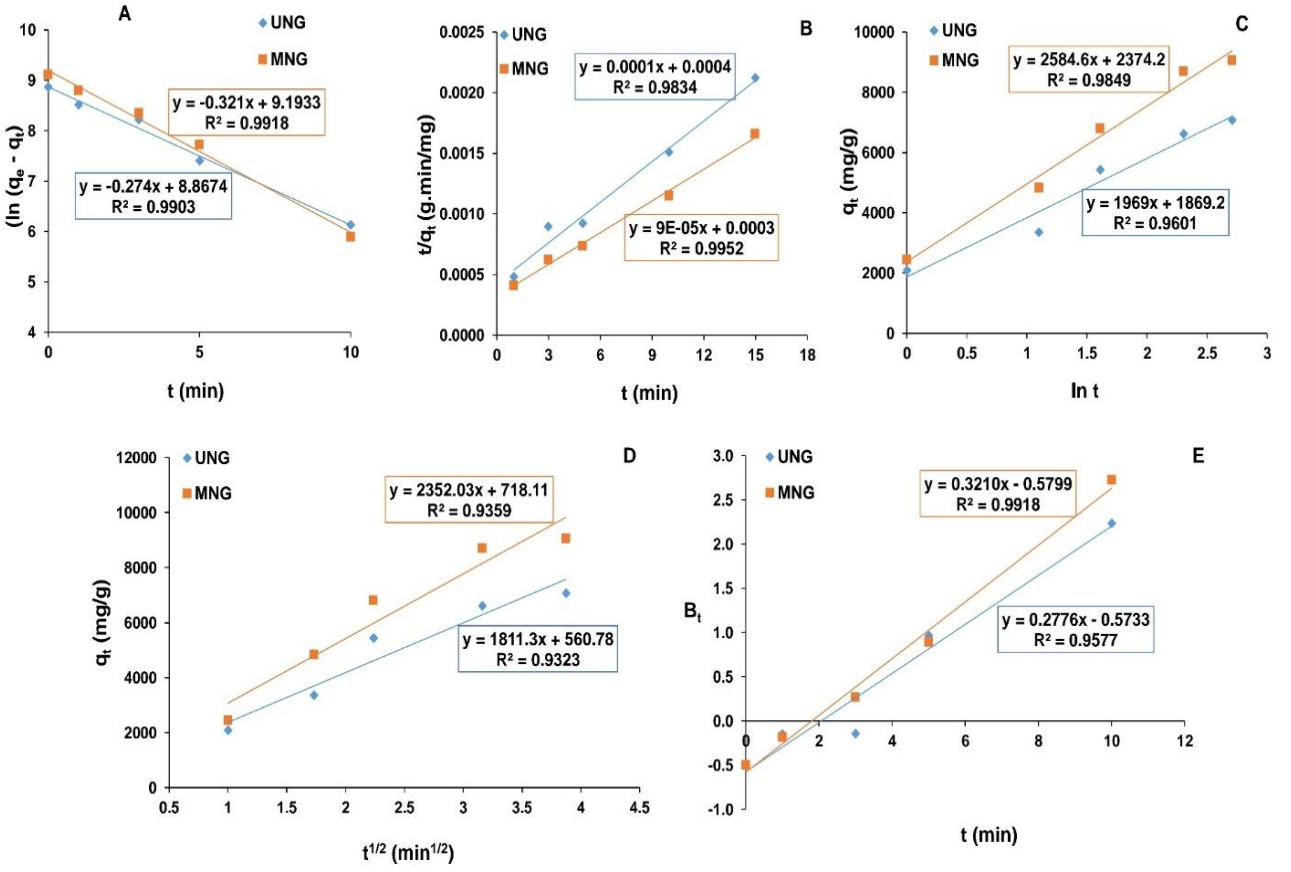

Figure 9. (a) Pseudo-First-order, (b) Pseudo-second-order, (c) Elovich, (d) intra-particle, and (e) Boyd Plots for Oil Sorption on Unmodified and Modified Napier Grass

Table 2. Kinetic Parameters for Oil Sorption on Unmodified and Modified Napier Grass

Parameter	UNG	MNG
q_e, exp (mg/g)	7070	9057
Pseudo-first-order model		
q_e (mg/g)	7097	9831
k_1 (min^{-1})	0.274	0.321
Pseudo-second-order model		
q_e (mg/g)	10000	11111
k_2 (g/mg·min)	2.03×10^{-5}	3.33×10^{-5}
The Elovich model		
β (g/mg)	5.08×10^{-4}	3.87×10^{-4}
α (mg/g·min)	5088	6476
Intra-particle diffusion model		
k_{id} ($mg/g \cdot min^{1/2}$)	1811.30	2352.03
C	560.78	718.11
Boyd model		
Intercept	−0.5733	−0.5799
Slope	0.2776	0.3210

Table 3. Comparison of the Crude Oil Sorption Capacities of Various Acetylated Agro-residues

Agro-residue	Oil sorption capacity (mg/g)	Reference
Corn silk	16680	[10]
Delonix regia pods	11570	[11]
Corn cob	5118	[12]
Sugarcane bagasse	9100	[13]
Oil palm empty fruit bunch	7160	[14]
Cocoa pods	7880	[14]
Dacryodes edulis leaf	5000	[15]
Modified Napier grass	9831	This work

Table 4. Paired Samples t-test for Oil Sorption Capacities of Unmodified and Modified Napier Grass

	Paired differences					t	df	Sig. (2-tailed)
	Mean	SD	SE Mean	95% CI of the difference				
				Lower	Upper			
Effect of adsorbent dose								
UNG - MNG	−1.20960	0.21619	0.06836	−1.36425	−1.05495	−17.693	9	0.000
Effect of the initial crude oil concentration								
UNG - MNG	−1.82480	0.57919	0.18316	−2.23913	−1.41047	−9.963	9	0.000
Effect of contact time								
UNG - MNG	−1.45510	0.65032	0.20565	−1.92031	−0.98989	−7.076	9	0.000

Statistical analysis. The results of the paired sample *t*-test (Table 4) reveal that statistically significant differences ($p < 0.05$) existed between the oil sorption capacities of MNG and UNG under different adsorption conditions (adsorbent dose, initial crude oil concentration, and contact time). This indicates that the modification process significantly improved the crude oil adsorption ability of Napier grass.

Conclusions

This study shows that Napier grass, which is a widely available agricultural resource, can be used to remove crude oil from aqueous media. Modification by mild acetylation effectively improved the sorption behavior of Napier grass. The oil sorption capacity of the modified grass was significantly higher than that of the unmodified grass under different adsorbent dose, initial crude oil concentration, and contact time conditions. Equilibrium analyses based on various isotherm models revealed that the adsorption data were best fit by the Langmuir, indicating that the crude oil coated the adsorbents as a monolayer. According to kinetic analyses, pseudo-first-order kinetics best described the adsorption processes, with equilibrium sorption capacities of 7097 and 9831 mg/g for UNG and MNG, respectively. The sorption processes were based on physisorption and controlled by film diffusion. These results suggest that the regeneration of the Napier grass would require an insignificant amount of energy, favoring its reuse. The high oil sorption capacity, low cost, biodegradability, and wide availability of acetylated Napier grass demonstrate its potential as a viable sorbent for oil spill mop-up applications.

Acknowledgments

The authors are grateful to the Department of Pure and Industrial Chemistry, Nnamdi Azikiwe University for supporting this research.

References

[1] Machałowski, T., Wysokowski, M., Petrenko, I., Fursov, A., Rahimi-Nasrabadi, M., Amro, M.M., *et al*. 2020. Naturally pre-designed biomaterials: Spider molting cuticle as a functional crude oil sorbent. J. Environ. Manag. 261: 110218, https://doi.org/10.1016/j.jenvman.2020.110218.

[2] Abdelwahab, O. 2014. Assessment of raw *luffa* as a natural hollow oleophilic fibrous sorbent for oil spill cleanup. Alex. Eng. J. 53(1): 213–218, https://doi.org/10.1016/j.aej.2013.11.001.

[3] Zang, D., Zhang, M., Liu, F., Wang, C. 2016. Superhydrophobic/superoleophilic corn straw fibers as effective oil sorbents for the recovery of spilled oil. J. Chem. Technol. Biotechnol. 91(9): 2449–2456, https://doi.org/10.1002/jctb.4834.

[4] El-Din, G.A., Amer, A.A., Malsh, G., Hussein, M. 2018. Study on the use of banana peels for oil spill removal. Alex. Eng. J. 57(3): 2061–2068, https://doi.org/10.1016/ j.aej.2017.05.020.

[5] Dong, T., Xu, G., Wang, F. 2015. Oil spill cleanup by structured natural sorbents made from cattail fibers. Ind. Crops Prod. 76: 25–33, https://doi.org/10.1016/ j.indcrop.2015.06.034.

[6] Ferreira, D.P., Cruz, J., Fangueiro, R. 2019. Surface modification of natural fibers in polymer composites. In Koronis, G., Silva, A. (eds.), Green Composites for Automotive Applications. Woodhead publishing. United Kingdom. pp. 3–41.

[7] Onwuka, J.C., Agbaji, E., Ajibola, V.O., Okibe, F. 2019. Thermodynamic pathway of lignocellulosic acetylation process. BMC Chem. 13: 79–90, https://doi.org/10.1186/s13065-019-0593-8.

[8] Yusof, N.A., Mukhair, H., Malek, E.A., Mohammad, F. 2015. Esterified coconut coir by fatty acid chloride as biosorbent in oil spill removal. BioResources. 10(4): 8025–8038, https://doi.org/10.15376/biores.10.4.8025-8038.

[9] Chen, J., Xu, J., Wang, K., Cao, X., Sun, R. 2016. Cellulose acetate fibers prepared from different raw materials with rapid synthesis method. Carbohydr. Polym. 137: 685–692, https://doi.org/10.1016/j.carbpol.2015.11.034.

[10] Asadpour, R., Sapari, N.B., Isa, M.H., Kakooei, S., Orji, K.U. 2015. Acetylation of corn silk and its application for oil sorption. Fibers Polym. 16: 1830–1835, https://doi.org/10.1007/s12221-015-4745-8.

[11] Onwuka, J.C., Agbaji, E., Ajibola, V.O., Okibe, F. 2016. Kinetic studies of surface modification of lignocellulosic Delonix regia pods as sorbent for crude oil spill in water. J. Appl. Res. Technol. 14(6): 415–424, https://doi.org/10.1016/j.jart.2016.09.004.

[12] Behnood, R., Anvaripour, B., Jaafarzadeh, N., Farasati, M. 2016. Oil spill sorption using raw and acetylated sugarcane bagasse. J. Cent. South Univ. 23: 1618–1625, https://doi.org/10.1007/s11771-016-3216-8.

[13] Nwadiogbu, J.O., Ajiwe, V.I.E., Okoye, P.A.C. 2016. Removal of crude oil from aqueous medium by sorption on hydrophobic corncobs: Equilibrium and kinetic studies. J. Taibah Univ. Sci. 10(1): 56–63, https://doi.org/10.1016/j.jtusci.2015.03.014.

[14] Onwuka, J.C., Agbaji, E.B., Ajibola, V.O., Okibe, F.G. 2018. Treatment of crude oil contaminated water with chemically modified natural fiber. Appl. Water Sci. 8: 86, https://doi.org/10.1007/s13201-018-0727-5.

[15] Nnaji, N.J.N., Onuegbu, T.U., Edokwe, O., Ezeh, G.C., Ngwu, A.P. 2016. An approach for the reuse of *Dacryodes edulis* leaf: Characterization, acetylation and crude oil sorption studies. J. Environ. Chem. Eng. 4(3): 3205–3216, https://doi.org/10.1016/j.jece.2016.06.010.

[16] Sawasdee, V., Pisutpaisal, N. 2014. Feasibility of Biogas Production from Napier Grass. Energy Proc. 61: 1229–1233, https://doi.org/10.1016/j.egypro.2014.11.1064.
[17] Alaneme, K.K., Olusegun, S.J., Alo, A.W. 2016. Corrosion inhibitory properties of elephant grass (*Pennisetum purpureum*) extract: effect on mild steel corrosion in 1M HCl solution. Alex. Eng. J. 55(2): 1069–1076, https://doi.org/10.1016/j.aej.2016.03.012.
[18] Nwadiogbu, J.O, Okoye, P.A.C., Ajiwe, V.I.E., Nnaji, N. 2014. Hydrophobic treatment of corncob by acetylation: Kinetics and thermodynamics studies. J. Environ. Chem. Eng. 2(3): 1699–1704, https://doi.org/10.1016/j.jece.2014.06.003.
[19] Mahmoud, M.A. 2020. Oil spill cleanup by waste flax fiber: modification effect, sorption isotherm, kinetics and thermodynamics. Arab. J. Chem. 13(6): 5553–5563, https://doi.org/10.1016/j.arabjc.2020.02.014.
[20] Sihombing, R., Krisnandi, Y.K., Widya, R., Luthfiyah, S.Z., Yunarti, R.T. 2015. Adsorption of Phosphate Ion in Water with Lithium-Intercalated Gibbsite. Makara J. Sci. 19(4): 131–136, https://doi.org/10.7454/mss.v19i4.5166.
[21] Shikuku, V.O., Mishra, T. 2021. Adsorption isotherm modeling for methylene blue removal onto magnetic kaolinite clay: a comparison of two parameter isotherms. Appl. Water Sci. 11: 103, https://doi.org/10.1007/s13201-021-01440-2.
[22] Bello, O.S., Chris, T., Oluwakemi, A., Alao, C. 2020. Sequestering a non-steroidal anti-inflammatory drug using modified orange peels. Appl. Water Sci. 10: 172, https://doi.org/10.1007/s13201-020-01254-8.
[23] Shin, H.S., Kim, J. 2016. Isotherm, kinetic and thermodynamic characteristics of adsorption of paclitaxel onto Diaion HP-20. Process Biochem. 51(7): 917–924, https://doi.org/10.1016/j.procbio.2016.03.013.
[24] Kaur, S., Rani, S., Mahajan, R.K., Asif, M., Gupta, V.K. 2015. Synthesis and adsorption properties of mesoporous material for the removal of dye safranin: kinetics, equilibrium, and thermodynamics. J. Ind. Eng. Chem. 22: 19–27, https://doi.org/10.1016/j.jiec.2014.06.019.
[25] Venkatesan, G., Rajagopalan, V. 2016. Adsorption kinetic models for the removal of Cu (II) from aqueous solution by clay liners in landfills. Int. J. Environ. Sci. Technol. 13: 1123–1130, https://doi.org/10.1007/s13762-016-0951-1.
[26] Oladimeji, A.S., Uzoamaka, I.E.M., Chidi, O. 2019. Decontamination of Ni(II) and Co(II) ions from Aqueous Medium using the Cola Lepidota Pericarp. Makara J. Sci. 23(1): 51–64, https://doi.org/10.7454/mss.v23i1.10865.
[27] Wekoye, J.N., Wanyonyi, W.C., Wangila, P.T., Tonui, M.K. 2020. Kinetic and equilibrium studies of Congo red dye adsorption on cabbage waste powder. Environ. Chem. Ecotoxicol. 2: 24–31, https://doi .org/10.1016/j.enceco.2020.01.004.
[28] Thompson, C.O., Ndukwe, A.O., Asadu, C.O.2020. Application of activated biomass waste as an adsorbent for the removal of lead (II) ion from wastewater. Emerg. Contam. 6: 259–267, https://doi.org/10.1016/j.emcon.2020.07.003.
[29] Akinterinwa, A., Oladele, E., Adebayo, A., Ajayi, O. 2020. Removal of Pb2+ and Cd2+ from Aqueous Solutions using POCl3 Cross-linked Carboxymethyl Derivatives of Legume Starch. Makara J. Sci. 24(3): 154–171, https://doi.org/10.7454/mss.v24i3.1201.
[30] Kumar, P.S., Senthamarai, C., Durgadevia, A. 2014. Adsorption kinetics, mechanism, isotherm, and thermodynamic analysis of copper ions onto the surface modified agricultural waste. Environ. Prog. Sustain. Energy. 33(1): 28–37, https://doi.org/10.1002/ep.11741.
[31] Zhang, Y., Shao, D., Yan, J., Jia, X., Li, Y., Yu, P., *et al*. 2016. The pore size distribution and its relationship with shale gas capacity in organic-rich mudstone of Wufeng-Longmaxi Formations, Sichuan Basin, China. J. Nat. Gas Geosci. 1(3): 213–220, https://doi.org/10.1016/j.jnggs.2016.08.002.
[32] Asadpour, R., Sapari, N.B., Isa, M.H., Orji, K.U. 2014. Enhancing the hydrophobicity of mangrove bark by esterification for oil adsorption. Water Sci. Technol. 70(7): 1220–1228, https://doi.org/10.2166/wst.2014.355.
[33] Chand, N., Fahim, M. 2021. Natural fibers and their composites. In Chand, N., Fahim, M. (eds.), Tribology of Natural Fiber Polymer Composites, 2nd ed. Woodhead publishing. United Kingdom. pp. 1–59.
[34] Purwaningrum, W., Vilantina, V., Rizki, W.T., Desnelli, D., Hariani, P.L., Said, M. 2021. Cr(III)-Doped Bentonite: Synthesis, Characterization and Application for Phenol Removal. Makara J. Sci. 25(2): 69–78, https://doi.org/10.7454/mss.v25i2.1171.
[35] Mohadi, R., Siregar, P.M.S.B.N., Palapa, N.R., Lesbani, A. 2022. Preparation of Zn/Al-chitosan Composite for the Selective Adsorption of Methylene Blue Dye in Water. Makara J. Sci. 26(2): 128–136, https://doi.org/10.7454/mss.v26i2.1313.
[36] Djayanti, S., Kusumastuti, S.A., Fatkhurrahman, J., Purwanto, A., Budiarto, A., Suherman, A.L. 2021. Synthesis and Characterization of Cellulose Acetate Membrane from Cotton Spinning Waste. Makara J. Sci. 25(3): 155–161, https://doi.org/10.7454/mss.v25i3.1219.
[37] Zheng, W., Sun, C., Bai, B. 2017. Molecular dynamics study on the effect of surface hydroxyl groups on three-phase wettability in oil-water-graphite systems. Polymers. 9(8): 370–379, https://doi.org/10.3390/polym9080370.

[38] Omer, A.M., Khalifa, R.E., Tamer, T.M., Ali, A.A., Ammar, Y.A., Eldina, M.S.M. 2020. Kinetic and thermodynamic studies for the sorptive removal of crude oil spills using a low-cost chitosan-poly (butyl acrylate) grafted copolymer. Desalin. Water Treat. 192: 213–225, https://doi.org/10.5004/dwt.2020.25704.

[39] Dawodu, F.A., Akpomie, K.G. 2014. Simultaneous adsorption of Ni (II) and Mn (II) ions from aqueous solution onto a Nigerian kaolinite clay. J. Mater. Res. Technol. 3(2): 129–141, https://doi.org/10.1016/j.jmrt.2014.03.002.

[40] Anuzyte, E., Vaisis, V. 2018. Natural oil sorbents modification methods for hydrophobicity improvement. Energy Proc. 147: 295–300, https://doi.org/10.1016/j.egypro.2018.07.095.

[41] Asadpour, R., Sapari, N.B., Isa, M.H., Kakooei, S. 2016. Acetylation of oil palm empty fruit bunch fiber as an adsorbent for removal of crude oil. Environ. Sci. Pollut. Res. 23: 11740–11750, https://doi.org/10.1007/s11356-016-6349-2.

[42] Mahdi, Z., El-Hanandeh, A., Yu, Q. 2017. Influence of Pyrolysis Conditions On Surface Characteristics and Methylene Blue Adsorption of Biochar Derived from Date Seed Biomass. Waste Biomass Valor. 8: 2061–2073, https://doi.org/10.1007/s12649-016-9714-y.

[43] Diraki, A., Mackey, H.R., McKay, G., Abdala, A.A. 2018. Removal of oil from oil–water emulsions using thermally reduced graphene and graphene nanoplatelets. Chem. Eng. Res. Des. 137: 47–59, https://doi.org/10.1016/j.cherd.2018.03.030.

[44] Rahangdale, D., Kumar, A. 2018. Chitosan as a substrate for simultaneous surface imprinting of salicylic acid and cadmium. Carbohydr. Polym. 202: 334–344, https://doi.org/10.1016/j.carbpol.2018.08.129.